Engineering Science and Technology, an International Journal 18 (2015) 769–775

HOSTED BY

Contents lists available at ScienceDirect

Engineering Science and Technology, an International Journal

journal homepage: http://www.elsevier.com/locate/jestch

Full length article

Investigation of ferrocement channels using experimental and finite element analysis

Hamid Eskandari*, Amirhossein Madadi

Department of Civil Engineering, Hakim Sabzevari University, Sabzevar, Iran

ARTICLE INFO

Article history:
Received 25 December 2014
Received in revised form
9 May 2015
Accepted 20 May 2015
Available online 19 June 2015

Keywords:
Ferrocement channel
Experimental analysis
Finite element analysis

ABSTRACT

It is necessary to design and calculate tensile reinforcement for ferrocement channels with various spans used in different structures such as rural houses and mosques. However, such analysis is challenging due to the application of different types of wire meshes, dissimilar tensile and compressive reinforcement, and mechanical properties of the mortar. The present study provided an experimental sample to assess deflection in a standard ferrocement channel (span: 4.5 m; width: 70 cm). The Abaqus Unified finite element analysis (FEA) has been also used to model the ferrocement channel by various system supports and beam spans. The obtained results indicated the acceptable accuracy of FE simulations in the estimation of experimental values. Such models can thus be used as quick, simple, and inexpensive methods to calculate the optimal deflection of ferrocement channels for various spans and sizes of tensile reinforcement.

1. Introduction

Ferrocement, also called reinforced concrete, is obtained by mixing cement with sand mortar and applying the mixture over some layers of woven [1] or welded [2] steel mesh with small-diameter holes [3]. It is widely used in shipbuilding [4–7], water and food storage tanks [8,9], water transport tubing [10], silos [11], roofs [12–15], urban and rural houses [16], and structure repair [17–19]. Ferrocement is especially popular because its raw materials are available, it is easy to prepare and shape, and it is fire resistant [20,21]. It is also known to promote the seismic resistance of masonry structures [22]. Research has indicated the use of additives such as fibers [23–25], silica [26–28], fly ash [29], and resin [30] to increase the strength of mortar in ferrocement. Other experimental studies have also suggested the applicability of polymer fibers instead of meshes in ferrocement. Moreover, ferrocement slabs are used as secondary roof structures to insulate against heat [31], in the manufacture of beams [32–36], and in building components such as doors [37] and drywalls [38]. The mechanical behavior of ferrocement elements such as beams, slabs, and columns has been examined under applied loads up to failure by experimental models such as Hago et al. [12] and Ibrahim [39] who studied experimentally the ultimate capacity of simply supported slab panels and ferrocement slabs.

Although the need for experimental research to provide the basis for design equations continues but by applying the FEM, can reduce the time and cost of otherwise expensive experimental tests, and may better simulate the loading and support conditions of the actual structure. So to this end the FEM is used by Nassif and Najm [40] to investigate the behavior of ferrocement composite beams under a two-point loading system. They used a smeared crack model, which can be applied the constitutive equations independently at each integration point of the model to determine failure in concrete and as a result they found that the ferrocement composite beams have better ductility, cracking strength, and ultimate capacity compared to reinforced concrete beams. Likewise Qasim Mohammad [41] studied the FEM to analyze the ferrocement slabs. Modeling of concrete compression and tensile cracking has been done by a plasticity model and smeared cracking approach respectively. Moreover, to study the composite action between the ferrocement slabs and steel sheeting, Aboul-Anen et al. [42] applied ANSYS software with Eight-node solid isoparametric elements. This finite element software was also used by Shaheen et al. [8] to find the modal parameters of the healthy and damage tank.

* Corresponding author. Tel.: +98 51 44013386; fax: +98 51 44012773.
E-mail address: Hamidiisc@yahoo.com (H. Eskandari).
Peer review under responsibility of Karabuk University.

http://dx.doi.org/10.1016/j.jestch.2015.05.008

In the current research, a finite element simulation was implemented using Abaqus Unified FEA (Dassault Systèmes, France) [43] to evaluate the experimental work. This software consists of variable procedures that allows for the implementation of specific material models (ferrocement/concrete and steel), boundary conditions, bond behavior and the interaction between the reinforcing steel and concrete. The software has an extensive library of elements that can be used to model concrete and reinforcement and in this numerical analysis in order to achieve more compatible experimental and analytical results, a three-dimensional brick element and a beam element, both in linear geometry were considered for modeling the ferrocement mortar and reinforcement respectively. These models were also developed to determine the optimal span of ferrocement channel under various uses (e.g. roof and floor) with different maximum (ultimate) loads. In addition, two types of support channels were investigated to obtain the optimal tensile reinforcement for channel in direction of the Y axis.

2. Channel design based on ferrocement

The design strength of all sections of ferrocement structures and structural members should be at least equal to the required strengths for the factored load and load combinations stipulated in the American Concrete Institute's Building Code Requirements for Structural Concrete (ACI) 318 [44]. Design strength provided by a member or a cross-section is expressed in terms of axial load, bending moment, shear force, or stress. The values shall be taken as the nominal strength, calculated based on the requirements and assumptions of the ACI 318, multiplied by the strength reduction factor Ø. The aim would be to satisfy the general relationship $U \leq Ø\ N$; where U is the factored load (equal to the minimum required design strength), N is the nominal resistance, and Ø is the strength reduction. Design strength for the mesh reinforcement should be based on the yield strength (fy) of the reinforcement but should not exceed 690 MPa [11].

The values of parameters used in calculations are presented in Table 1.

2.1. Volume fraction of reinforcement (V_f)

V_f is the total volume of reinforcement divided by the volume of composite (reinforcement and matrix) and can be obtained from the following equation:

$$V_f = \frac{N\pi d_b^2}{4h}\left(\frac{1}{D_l}+\frac{1}{D_t}\right) = 0.637\% \quad (1)$$

2.2. Effective area of reinforcement (A_{si})

The area of reinforcement per layer of mesh is considered effective to resist tensile stresses in a cracked ferrocement section. A_{si} can be determined as:

$$A_{si} = \eta V_{fi}\ A_c = 4.78 \times 10^{-5}\left(m^2\right) \quad (2)$$

When multiplied by the volume fraction of reinforcement, the global efficiency factor η gives the equivalent volume fraction (or equivalent reinforcement ratio) in the loading direction considered.

2.3. Nominal tensile strength (N_n)

The nominal resistance of cracked ferrocement elements subjected to pure tensile loading can be approximated by the load-carrying capacity of the mesh reinforcement alone in the direction of loading. The following procedure may be used:

$$N_n = A_s f_y = 82(KN) \quad (3)$$

2.4. Nominal moment strength (M_n)

If vibrating the compressive strength of ferrocement is considered 2 MPa; then M_n can be obtained through the following equation:

$$M_n = \sum_{i=1}^{n} C_{si} or T_{si}\left(d_i - \frac{\beta_1 c}{2}\right) = 2.9(KN.m) \quad (4)$$

where:

M_n = nominal moment strength;
C_{si} = the internal compressive force provided by the longitudinal reinforcing layer i;
T_{si} = the internal tensile force provided by the longitudinal reinforcing layer i;
di = distance from the extreme compression fiber to the centroid of reinforcing layer i;
β_1 = the factor defining the depth of the rectangular stress block; and
c = distance from the extreme compression fiber to the neutral axis.

3. Materials and methods

3.1. Materials and mixing proportions

Type II ordinary portland cement (OPC) was provided by Torbat and Sabzevar Cement Factories (Iran). The ferrocement mortar was

Table 1
Parameters used in ferrocement channel design.

Parameter	Definition	Value
B	Width of the ferrocement section	1 (m)
H	Thickness of the ferrocement section	0.05 (m)
N	Number of mesh layers (nominal resistance)	2
F_y	yield strength of mesh reinforcement or reinforcing bars	2400 (kg/cm^2)
W_m	Unit weight of mesh	0.5 (kg/m^2)
γ_m	Density of steel	7850 (kg/m^3)
d_b	Diameter of mesh wire	0.8×10^{-3} (m)
D_l	Center-to-center spacing of wires aligned longitudinally in the reinforcing mesh	0.06 (m)
D_t	Center-to-center spacing of wires aligned transversely in the reinforcing mesh	0.06 (m)
A_s	Total effective cross-sectional area of bonded reinforcement	352×10^{-6} (m^2)
η	Global efficiency factor of embedded reinforcement in resisting tension or tensile-bending loads	0.3
A_c	Cross-sectional area of the ferrocement composite	0.05 (m^2)

Table 2
Mixing proportions applied to produce the ferrocement channel.

Mix design	Cement (kg/m^3)	Fine aggregate (kg/m^3)	Water/cement	Superplasticizer (kg/m^3)
I	800	1600	0.5	–
II	800	1600	0.3	8

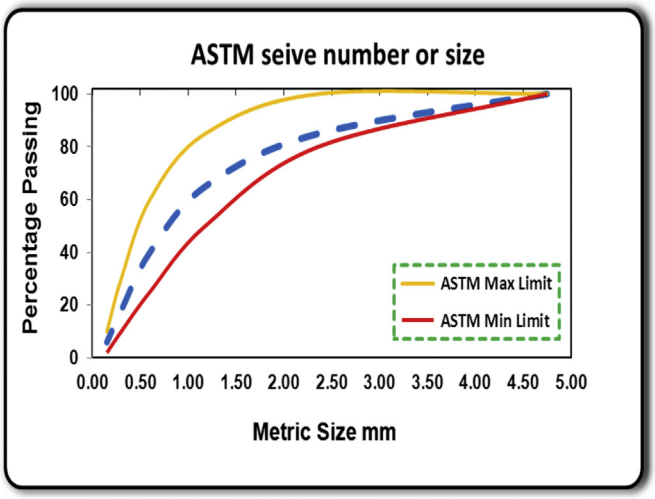

Fig. 1. Sieves analysis of fine aggregate for ferrocement.

made with natural clean sand with a cement/sand ratio of 1:2. Fresh drinking water was also added with a water/cement ratio of 0.5:0.3 (Table 2). Moreover, sieve analysis was performed on the used sand (Fig. 1).

The mixtures were cast in 100 × 100 mm cubes and tested under compression loadings after 28 days. Accordingly, the compressive strength of the cement from Torbat and Sabzevar Cement Factories was calculated as 45 and 25 MPa, respectively.

The chicken and expanded meshes (Fig. 2) were employed in the experimental work. In addition to meshing, three longitudinal re-bars (an Ø10 mm rebar for top and two Ø12 mm ones for bottom of the channel) were used.

3.2. Specimen preparation and testing

The construction process involved molding to create the desired shape of channels (Fig. 3). Afterward, a plastic cover was placed under the mortar mix. While the initial cover of the channel mortar was approximately 2 cm, it reached 5 cm after placing the meshes and the reinforcement. Ultimately, the entire surface of the channel was completely covered and smoothed.

In order to measure deflection, two-point flexure tests were conducted on the specimens after appropriate curing for 28 days. The two sides of the channels were fixed by profiles to provide hinge support (Fig. 4).

3.3. Finite element analysis

A general-purpose code, Abaqus Unified FEA which is a finite element based software and a powerful tool to investigate the behavior of the proposed ferrocement channels, was applied in this study. Several elements are available which can be used to model reinforced concrete in this program and from a variaty of elements

Fig. 2. Reinforcement steel meshes.

Fig. 3. Sample preparation.

Fig. 4. Type of support and flexural test.

an 8-node linear brick element with reduced integration (Type C3D8R) and a 2-node linear beam (Type B31) due to the better satisfying the boundary conditions along the elements borders and closer results of analytical and exprimental models, were considered for modeling the mortar of ferrocement and reinforcement respectively. It had three degrees of freedom at each node (translations in the nodal X, Y, and Z directions). The ferrocement mortar was modeled with concrete charactristics using elastic modulus of (Ec) 2 GPa and poisson's ratio of 0.2 and these values for reinforcement were 200 GPa and 0.3 respectively. In addition, deformable solid shape in the 3-D modeling space through extrusion type and 3-D planar deformable body and a wire base feature were used to represent the mortar of ferrocement and the reinforcement respectively. Model was developed for a fixed, hinged and roller supported samples of 4.5 and 9 m under the surface loads of 200 and 300 kg/m^2.

4. Implementation, results and challenges

4.1. Evaluation of concrete and various meshes on ferrocement roofs

As mentioned earlier, the samples were made with two different kinds of cement sand mortar and various meshing. In the second mortar, the water/cement ratio was reduced to 0.3 (vs. 0.5 in the first mortar). Moreover, 1% superplasticizer was added to the

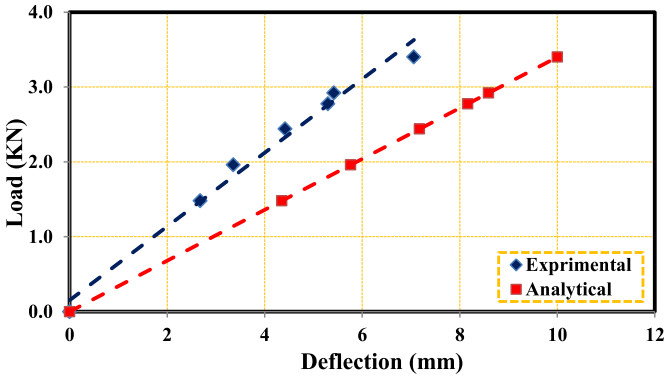

Fig. 6. Load-deflection relationships in the experimental and finite element (FE) models.

mortar to increase plasticity. In order to enhance mortar performance and facilitate construction, sand particle size was determined based on the relevant administrative laws. On the other hand, finer particle size of Torbat cement compared to Sabzevar cement resulted in its softer texture and higher adhesion not only to its own components, but also to the mesh and steel bars.

The sectional area of reinforcement and the resultant tensile force and moment were first calculated according to the ACI-549. The constructed samples had four different mesh cross-sections. Some samples without the required reinforcement cross-section lacked adequate resistance in the tests and thus failed at their critical points (Fig. 5). Shear cracking also occurred at different parts, especially near the steel bars on the two sides of the samples. Increasing the number of layers or reinforcing the mesh can generally improve the flexural capacity of the cross-sections. Finally, combination of expanded metal lath with wire mesh would lead to better results.

4.2. Comparison of the experimental and FE models

Load deflection from the lateral edge of the channel under flexural strength under two-point loading in the experimental model is shown in Fig. 6. Although various parameters can affect load deflection, only the linear load is applied in the FE model. Comparison between the developed FE model of the channel and the findings from the experimental model suggested that the two models yielded similar trends. As regards the ferrocement channel is 5 cm thickness and there is no vibration used in construction operations the variant of modulus of elasticity is sensitive to FE model. Therefore, with a reliable factor of safety and optimal designing the trend may be acceptable.

Fig. 5. Samples constructed with two types of meshes.

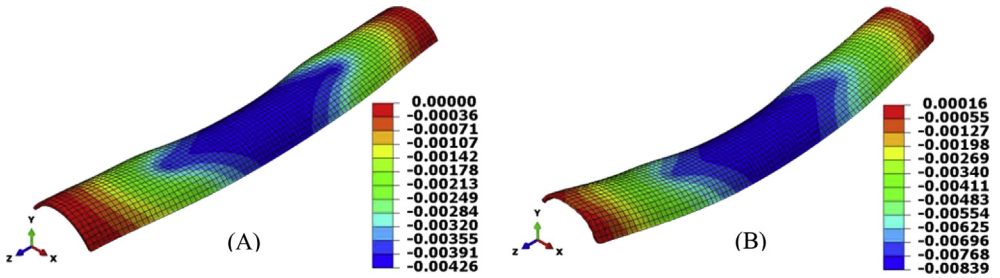

Fig. 7. The finite element (FE) model of deformation in the Y axis for the 4.5 m sample with fixed (A) and hinge support (B). All units are in (m).

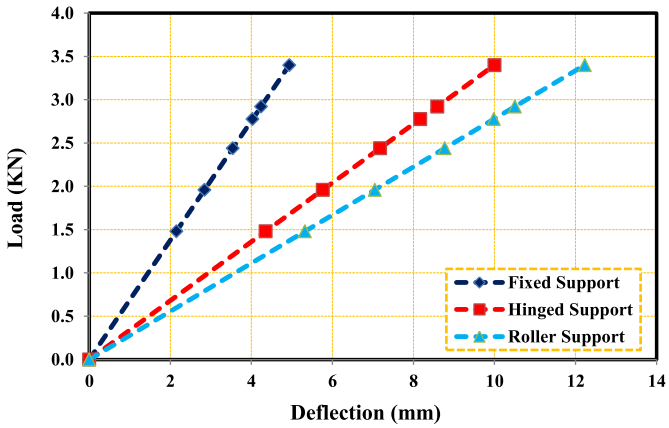

Fig. 8. Load vs. deflection of the finite element (FE) models.

The FE model have been developed for three types of fixed, hinge, and roller supports which for the first two ones shown in Fig. 7.

The deflection results for 2.5 KN two-point load and for fixed and hinge supports are shown in Fig. 8 due to their more importance and application. As seen, deflections at the midspan of the hinge support were almost twice that in the fixed support. Moreover, midspan deflections in the Y direction of the hinge and roller supports were closer to each other than to that of the fixed support. Furthermore, due to the absence of a particular design for this type of channel, the effects of type of support on channel deflection (presented in Fig. 8) can be beneficial for the approximate deflection of channel in construction.

In addition, the FE models are developed for continuous supports with 4.5 m spans. The deflection values of these contours by two types of fixed (A) and hinge (B) cross-sections are depicted in Fig. 9. By scrutinizing these models, it can be concluded that the maximum deflection for hinge support is about 10% more than that of fixed support. However, comparing these results with previous models for one 4.5 m span revealed that the values of maximum deflections are about four and six times less than the one-span models for fixed and hinge supports, respectively. Therefore, the deflection quantities could be controlled in allowable limits by enhancing the supports and the number of spans.

Fig. 10 compares the three types of supporters by investigating the deflections in the X, Y and Z axes for continuing channels. In the X axis, a gross difference in deflection of the channel was observed for the roller support. However, the values in the fixed and hinge supports were almost similar. Deformation of the channels in the Y axis (shown in the FE models) indicated an association between decreased support constraints and increased deflection. While similar results were detected in the Z axis, using fixed supporters in the cross-section caused very low deformation between points 2 and 4 and more at points 1 and 5.

In order to optimize the deflection, a total of 72 FE models with different sizes of the bottom channel reinforcement (6, 8,10, 12, 14, and 16 mm), and load types (200 and 300 kg/m^2), and channel lengths (3, 4, 5, 6, 7, and 8 m) were analyzed (Fig. 11). As seen, an increase in length resulted in increased deflection and size of reinforcement. Furthermore, a higher load was associated with higher deflection. Meanwhile, the difference between the amounts of deflection under different loads was greater in higher lengths of channels. In addition, a greater load on the structure increased the maximum deflection. Such an increment was more obvious in longer samples. At a particular length, on the other hand, increasing the diameter of the bars decreased the deflection. However, the deflection was less affected by rebar diameter than by channel length. The optimal design is the graph's intersection of length and rebar diameter. For instance, under a load of 300 kg, the optimal design would have a rebar diameter of Ø12 and a channel length of 3.5 m.

5. Conclusion

In this study, experimental samples were designed and constructed with various materials (e.g. meshes and mortar) and an optimal combination of meshes has been obtained then the FE

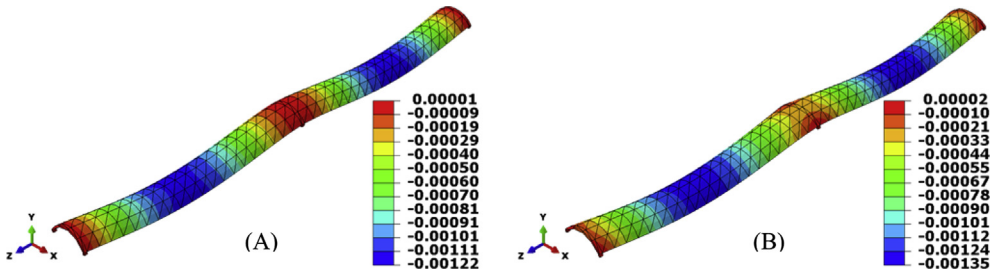

Fig. 9. The finite element (FE) model deformation in the Y axis for the 9 m sample in fixed (A) and hinge support (B). All units are in (m).

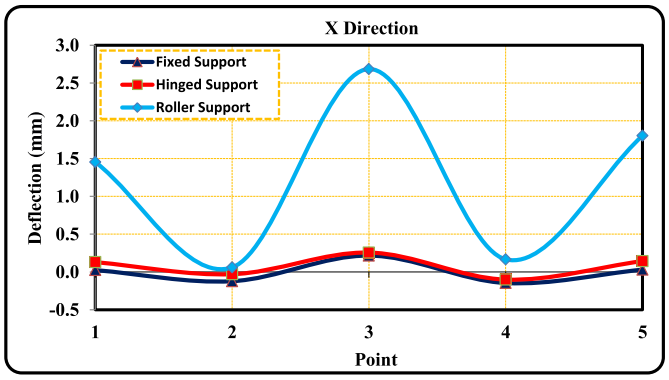

(A)

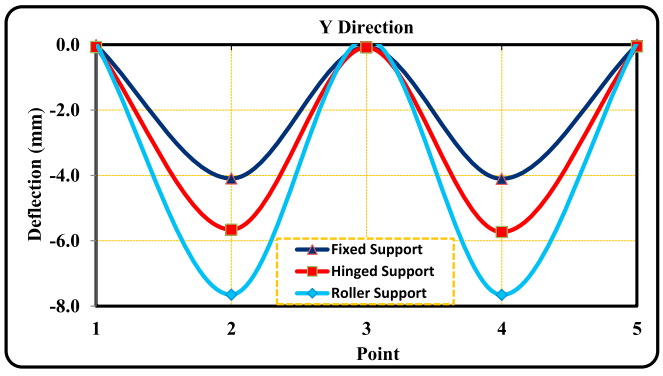

(B)

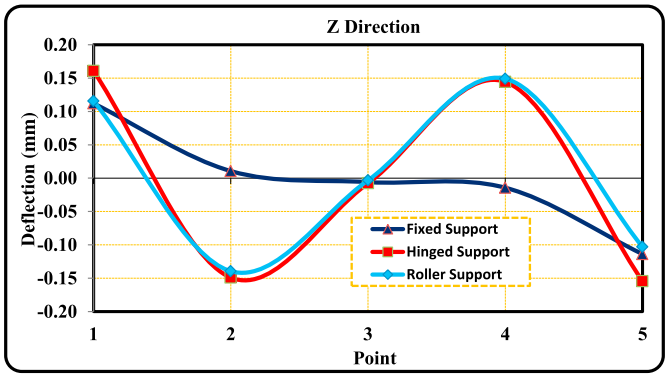

(C)

Fig. 10. Shape of deflections in the X (A), Y (B), and Z directions (C) for the 9 m finite element (FE) models using various supports.

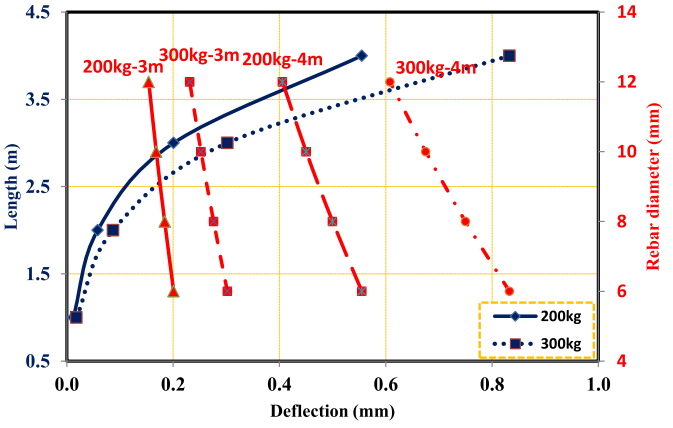

(A)

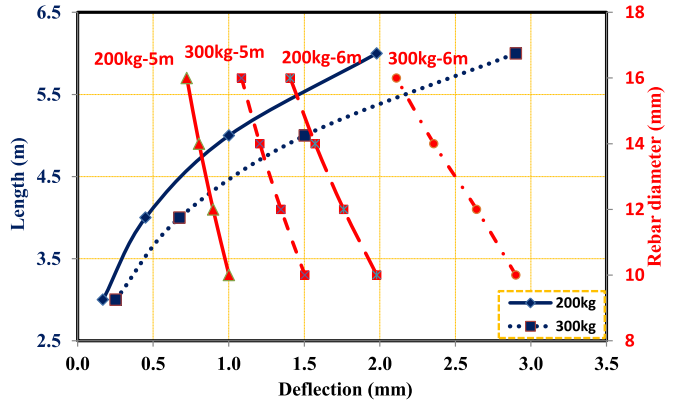

(B)

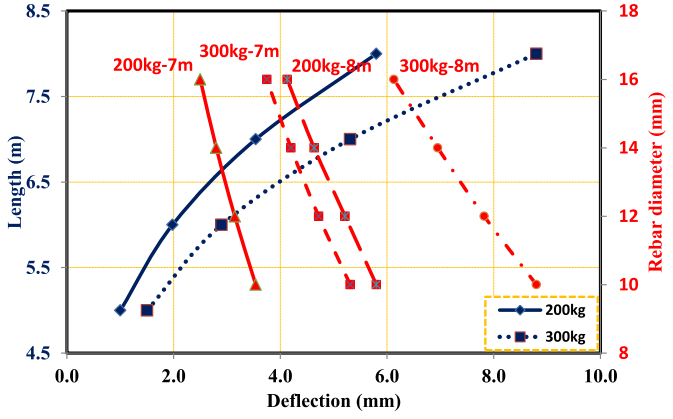

(C)

Fig. 11. Finite element (FE) models of the relationship between length, deflection, and rebar diameter under 200 and 300 kg/m^2 loads.

models of the channel were implemented using Abaqus Unified FEA. The models can be used to obtain optimal span of ferrocement channels in different applications (such as roofs and floors) which have unalike maximum loads. In addition, two types of support channels were investigated to determine the optimal tensile reinforcement for the channel in direction of the X and Y axes. Our findings indicated that:

1. A combination of meshes (expanded metal lath with wire mesh) with water/cement = 0.5 and Torbat cement provided a better design for construction.
2. The FE models could be applied for various support types of the cross-sections. Meanwhile, fixed support was the most effective in minimizing the deflection.
3. Finally, this implementation could be used for designing the optimal lengths for constant rebar diameters.

References

[1] A.A. Skudra, Eastic characteristic of ferrocement reineforced with woven meshes, Mech. Compos. Mater. 30 (4) (1994) 382–385.
[2] G. Singh, G.J. Xiong, A study of ultimate moment capacity of ferrocement reinforced with weld mesh, Cem. Concr. Compos. 14 (4) (1992) 257–267.
[3] ACI Committee 549, Report on Ferrocement, Concrete International. USA 87, 2009.
[4] Naval Ship Systems Command, U.S. NAVY Ferrocement Boat Building Manual (1–3), Washington, D. C, 1972.

[5] F.S. Hespe, H.T. Kami, R.K. Sakamoto, Ferro-cement Shell Hull Construction for Fishing Boats, South Pacific Commision, Fourth Technical Meeting on Fisheries, Noumea, New Caledonia, 1970.
[6] F.E. BRAUER, Ferrocement for boats and crafts, Nav. Eng. J. 85 (5) (1973) 93–105.
[7] A.W. Greenius, Ferrocement for Canadian Fishing Vessels: A Summary and Interpretation of Test Results 1969 1974, Industrial Development Branch, Fisheries and Marine Service, Environmental Canada, Ottawa, 1975.
[8] Y.B.I. Shaheen, B. Eltaly, M. Kamel, Damage detection of ferrocement tanks using experimental modal analysis and finite element analysis, Concr. Res. Lett. 4 (2) (2013).
[9] Y.B.I. Shaheen, B. Eltaly, M. Kamel, Experimental and analytical investigation of ferrocement water pipe, J. Civ. Eng. Constr. Technol. 4 (4) (April, 2013) 157–167.
[10] National Academy of Sciences, Ferrocement: Applications in Developing Countries, Washington, D.C, Feb 1973.
[11] ACI Committee 549, Guide for Design, Construction and Repair of Ferrocement, ACI 549 IR-881989, 1989.
[12] A.W. Hago, K.S. Al-Jabri, A.S. Alnuaimi, H. Al-Moqbali, M.A. Al-Kubaisy, Ultimate and service behavior of ferrocement roof slab panels, Constr. Build. Mater. 19 (2005) 31–37.
[13] W.N. Al-Rifaie, M.M. Joma'ah, Structural behaviour of ferrocement system for roofing, in: Diyala Journal of Engineering Sciences, First Engineering Scientific Conference, College of Engineering-University of Diyala. December, 2010, pp. 237–248.
[14] V.C. NahroRadiHusein, AnupamRawat Agarwal, An experimental study on using lightweight web sandwich panel as a floor and a wall, Int. J. Innov. Technol. Explor. Eng. (IJITEE) 3 (7) (December 2013).
[15] Y. Yardim, A.M.T. Waleed, M.S. Jaafar, S. Laseima, AAC-concrete light weight precast composite floor slab, Constr. Build. Mater. 40 (2013) 405–410.
[16] W.N. Al-Rifaie, Modern housing system using ferrocement as sustainable construction materials, in: 7th. Municipal Work, Conference & Exibition, 24–26 April, Kingdom of Bahrain, 2012.
[17] K.M. Amanat, M.M.M. Alam, M.S. Alam, Experimental investigation of the use of ferrocement laminates for repairing masonry in filled RC frames, J. Civ. Eng. (IEB) 35 (2) (2007) 71–80.
[18] J.C. Adajar, T. Hogue, J. Colin, Ferrocement for hurricane- prone state of Florida, in: Structural Faults Repair- Conf, on June 13–15, Edinburgh, Scotland, UK, 2006.
[19] D. Rajkumar, B. Vidivelli, Performances of SBR latex modified ferrocement for repairing reinforced concrete beams, Aust. J. Basic Appl. Sci. 4 (3) (2010) 520–531.
[20] V. Greepala, P. Nimityongskul, Structural integrity of ferrocement panels exposed to fire, Cem. Concr. Compos. 30 (5) (2008) 419–430.
[21] Yousry Bl. Shaheen, G. Ramadan Ahmed, Pre-and post-fire strength assessment of ferrocement beams, Concr. Res. Lett. 3 (3) (2012).
[22] S. Shang, K. Liu, F. Yao, Rural residential seismic resistance practical technology, Earth Space 2010 (2010) 3368–3376.
[23] C. Soranakom, B. Mobasher, Correlation of tensile and flexural behavior of fiber reinforced cement composites, in: Ferro8, Proceedings of the 8th International Ferrocement and Thin Reinforced Cement Composites Conf, Bangkok, Thailand, 2006.
[24] M. Jamal Shannag, Tareq Bin Ziyyad, Flexural response of ferrocement with fibrous cementitious matrices, Constr. Build. Mater. J. 21 (2007) 1198–1205.
[25] S. DeepaShri, R. Thenmozhi, Flexural behavior of hybrid ferrocement slabs with microconcrete and fibers, J. Emerg. Trends Eng. Dev. 4 (2) (2012) 165–177.
[26] P. Rathish Kumar, High performance superplasticized silica fume mortars for ferrocement works, Int. J. FactaUniverstatis 8 (2) (2010) 129–134. Series Architecture and Engineering ISSN 0354–4605.
[27] M.A. Mashrei, G.M. Kamil, H.M. Oleiwi, High performance of silica fume mortars for ferrocement applications, Eng.
[28] A. Booshehrian, Effect of Nano-SiO_2 particles on properties of cement mortar applicable for ferrocement elements, Concr. Res. Lett. 2 (1) (2011) (March).-C.167-180.
[29] L. Andal, M.S. Palanichamy, M. Sekar, Strength and durability of polymer and fly ash modified ferrocement roofing/flooring elements, in: 33rd Conference on our world in concrete & structures: 25 – 27, 2008. Singapore. http://cipremier.com/100033009.
[30] Kumar, Acrylic rubber latex in ferrocement for strengthening reinforced concrete beams, Am. J. Eng. Appl. Sci. 3 (2) (2010) 277–285.
[31] V. Greepala, R. Parichatprecha, T. Tanchaisawat, P. Nimityongskul, Specific Heat Capacity of Ferrocement Using Inverse Thermal Analysis, RSID6- STR-10, 2009, http://fscieng.csc.ku.ac.th/~ce/images/stories/paper/vatwong_rsid_str10.pdf (accessed at 8–2011).
[32] B.P. Hughes, N.F.O. Evbuomwan, Polymer modified ferrocement enhances strength of reinforced concrete beams, Constr. Build. Mater. 7 (1) (1993) 9–12.
[33] P. Paramasivam, Ferrocement structural applications, National University of Singapore, Singapore 26th Conference on Our World in Concrete & Structures.
[34] B.I. Shaheen Yousry, Noha M. Soliman, Ashwaq M. Hafiz, Structural behaviour of ferrocement channels beams, Concr. Res. Lett. 4 (3) (2013).
[35] J.H.L. Bong, E. Ahmed, Study the structural behaviour of ferrocement beam, Unimals e-J. Civ. Eng. 1 (2) (2010).
[36] E.H. Fahmy, M.N.A. Zeid, Y.B. Shaheen, A. Abdelnaby, A permanent ferrocement forms: a viable alternative for construction of concrete beams, in: 30th Conference Our World in Concrete & Structures, Singapore, 2005.
[37] T. Baetens, Manufacturing and Specifications of Prefabricated of Ferrocement Doors, Auroville Building Centre – Ferrocement Doors, 2004.
[38] E.H. Fahmy, B.S. Yousry, Mohamed N. Abou AbouZeid, Hassan Gaafar, Ferrocement sandwich and cored panels for floor and wall construction, in: Proceedings of the 29th Conference on Our World in Concrete & Structures, Singapore, 2004.
[39] H.M. Ibrahim, Experimental investigation of ultimate capacity of wired mesh-reinforced cementitious slabs, J. Constr. Build. Mater. 25 (2011) 251–259.
[40] H.H. Nassif, H. Najm, Experimental and analytical investigation of ferrocement–concrete composite beams, J. Cem. Concr. Compos. 26 (2004) 787–796.
[41] I. Qasim Mohammad, Analysis of ferrocement slabs using finite element method, Basrah J. Eng. Sci. 12 (2) (2012) 14–19.
[42] B. Aboul-Anen, A. El-Shafey, M. El-Shami, Experimental and analytical model of ferrocement slabs, Int. J. Recent Trends Eng. 1 (6) (2009) 25–29.
[43] ABAQUS, Analysis User's Manuals and Example Problems Manuals, version 6.12, Abaqus Inc, Providence, Rhode Island.
[44] ACI Committee, Building Code Requirements for Structural Concrete (ACI 318-05) and Commentary (ACI 318R-05), American Concrete Institute, 2005.